Aalto University
School of Science
Department of Applied Physics

Aku Peltola

Trade off between the level of accuracy and required computational resources for hybrid functional NAO DFT calculations

Special Assignment Report

PHYS-E0441 — Physics Special Assignment V

Report submitted for approval: 24.8.2018

Supervisor: Senior University Lecturer Ville Havu

Instructor(s): Senior University Lecturer Ville Havu

Aalto University
School of Science

Aalto University, P.O. BOX 11000, 00076 AALTO
www.aalto.fi

Abstract of Physics Special Assignment

Author Aku Peltola

Title of the work Trade off between the level of accuracy and required computational resources for hybrid functional NAO DFT calculations

Degree programme Engineering Physics and Mathematics

Major Engineering Physics **Code of major** SCI3056

Supervisor Senior University Lecturer Ville Havu

Instructor(s) Senior University Lecturer Ville Havu

Date 24.8.2018 **Number of pages** iv+26 **Language** English

Abstract

Density functional theory (DFT) is a widely used theory for studying the electronic structure of matter [2]. Focus of this special assignment is on DFT-calculations performed via use of numerically tabulated atom-centered orbitals (NAOs) as implemented the Fritz Haber Institute "ab initio molecular simulations" (FHI-aims) computer program package.

The focus of this work is finding a balance between accuracy and use of the computational recourses. This problem arises especially for bigger periodic system calculations performed via use of the hybrid exchange–correlation functionals. This is done via producing new settings for the calculations called intermediate-settings. Simulations performed via use of the intermediate-settings should sit nicely between the pre-existing light- and the tight-settings in both level of convergence of the calculation and the computational resources used.

Three different methods were used while producing the new a intermediate settings for Na, K, Pt, Mo, Mn and Cr. First being decrease of the pool of basis functions, second being adjustment to confining-potential and third being use of auxiliary basis functions. The performance of the new intermediate-settings is verified in five different chemical environments and the accuracy should translate to other chemical environments as well.

Keywords DFT, NAO, set of basis functions, auxiliary basis function, xc-functional, HSE06

Contents

1 Introduction

The electronic structure of a quantum system determines the physical behavior of the system and hence determining the electronic structure is a major topic for the fields of chemistry, physics and material-science in general [1]. Density functional theory (DFT) is a widely used theory for studying the electronic structure of matter [2]. The focus of this special assignment is on DFT-calculations performed via use of the numerically tabulated atom-centered orbitals (NAOs) as implemented the Fritz Haber Institute "ab initio molecular simulations" (FHI-aims) computer program package.

Level of simplicity of the used DFT exchange-correlation (XC)-fuctional is defined by the Jacob's ladder which defines chemical accuracy of calculation [2]. Jacob's ladders are divided to five rungs with chemical accuracy increasing with computational recourses (time and memory) needed for the simulation under discussion [2]. The first rung is local density approximation (LDA), the second rung is generalized gradient approximation(GGA), the third rung, the metaGGA includes the local density, the gradient of the density and kinetic energy density. In the fourth rung called hyperGGA besides the local density and the gradient of the density, also exact exchange is included [2–4].

The focus of this work is finding a balance between accuracy and use of the computational recourses. This problem arises especially for bigger periodic system calculations performed via use of the hybrid exchange–correlation functionals which belong in the fourth rung of Jacob's ladder. This is done via producing new settings for the calculations called intermediate-settings. Simulations performed via use of the intermediate-settings should sit nicely between the pre-existing light- and the tight-settings in both level of convergence of the calculation and the computational resources used.

The calculations are performed via use of the hybrid functional (HSE06) and also via use of LDA in order to verify that for both functionals results for the new intermediate settings sit nicely between those of light- and tight-settings. Nothing drastic should occur for the elements considered in this work (Na, K, Pt, Mo, Mn and Cr). However experience with NAOs tells us that they will provide similar accuracy also in different chemical environments [5].

2 Background

2.1 DFT and ground state energy calculation

Density functional theory (DFT) is a widely used theory for studying electronic structure of materials. DFT is being used to calculate the electronic ground state density via minimization of the total energy. The DFT total energy of a system (nuclei and electrons) is

$$E_{tot} = T_s[n] + V_{ext}[n] + E_{es}[n] + E_{xc}[n] + E_{nuc-nuc}, \tag{1}$$

where T_s is the single particle kinetic energy, V_{ext} is the external potential generated by nuclei or external field, E_{es} is the Hartee energy generated by electrons, E_{xc} is the exchange-correlation energy and $E_{nuc-nuc}$ is the internuclear repulsion. Via use of the Born–Oppenheimer approximation the wavefunction can be broken to electronic- and nuclear parts. After this is done the nuclei are treated classically whereas the electronic part of the wavefunction is treated quantum mechanically [6]. After this is done n-electron many body systems can be reduced to n one-electron Kohn-Sham (KS) equations

$$\widehat{h}^{KS}|\psi_l = \epsilon_l|\psi_l. \tag{2}$$

Here $\widehat{h}^{KS}$ is the KS hamiltonian, ψ_l are the Kohn–Sham orbitals and ϵ_l are the eigenvalues. From here the electron density can be expanded as a sum of effective single-particle orbitals $|\psi_l$

$$n(\bar{\mathbf{r}}) = \sum_{l}^{N_{occ}} f_l|\psi_l|^2. \tag{3}$$

Here f_l varies from 0 to 1 depending on the occupation of the orbital. This is known as the eigenstate-based density update and it scales as $\mathrm{O}(N^2)$ [5, 6]. For larger systems it is favorable to use the density matrix based density update which comes from rewriting Eq. (3)

$$n(\bar{\mathbf{r}}) = \sum_{l}^{N_{occ}} f_l\psi_l^*\psi_l$$

and ψ_l can be expanded in terms of the basis functions

$$\psi_l(\bar{\mathbf{r}}) = \sum_i c_{il}\varphi_i(\bar{\mathbf{r}}), \tag{4}$$

where φ_i is a locally non-zero basis function and c_{il} is the corresponding coefficient. Now

$$n(\bar{\mathbf{r}}) = \sum_l f_l \sum_{ij} c_{il}^* c_{jl} \varphi_i^*(\bar{\mathbf{r}})\varphi_j(\bar{\mathbf{r}}) = \sum_{ij} \varphi_i(\bar{\mathbf{r}}) n_{ij} \varphi_j(\bar{\mathbf{r}}) \tag{5}$$

and when $c_{il}^*$and φ_i^* are real the density matrix is

$$n_{ij} = \sum_{l}^{N_{occ}} f_l c_{il} c_{jl}.$$

For localized basis functions the density matrix based density update scales as O(N) [5, 6].

The Kohn-sham single particle Hamiltonian arising from the minimization of Eq. (1) is

$$\widehat{h}^{KS} = \widehat{t}_s + \widehat{v}_{ext} + \widehat{v}_{es} + \widehat{v}_{xc}, \tag{6}$$

where $\widehat{t}_s$ is the single particle kinetic energy, $\widehat{v}_{ext}$ is the external potential generated by nuclei or external field, $\widehat{v}_{es}$ is the Hartee potential generated by electrons and $\widehat{v}_{xc}$ is the exchange-correlation potential. The electrostatic potential can be expanded as a sum over free atom potentials and a delta term

$$v_{es}(\bar{\mathbf{r}}) = \int \frac{n(\bar{\mathbf{r}}')}{|\bar{\mathbf{r}} - \bar{\mathbf{r}}'|} d^3r' = \sum_{at} v_{at}^{es,free}(|\bar{\mathbf{r}} - \bar{\mathbf{R}}_{at}|) + \delta v_{es}(\bar{\mathbf{r}}). \tag{7}$$

Here the term

$$\delta v_{es}(\bar{\mathbf{r}}) = \sum_{at,lm} \delta\tilde{v}_{at,lm}(|\bar{\mathbf{r}} - \bar{\mathbf{R}}_{at}|) Y_{lm}(\Omega_{at}) \tag{8}$$

is a sum of the electrostatic multipole potentials $\delta\tilde{v}_{at,lm}$ [6]. Parameter l_{max}^{es} works as a cutoff since the summing is done only up-to the order of l_{max}^{es}. During the calculation of $v_{es}(\bar{\mathbf{r}})$ the computational effort grows as $(l_{max}^{es})^2$ but l_{max}^{es} also has significant effect on the accuracy of calculation [5, 6].

Via discretization of Eq. (4) the Hamiltonian of Eq. (2) can be developed to the generalized eigenvalue problem

$$\sum_j h_{ij} c_{jl} = \epsilon_l \sum_j s_{ij} c_{jl}, \tag{9}$$

where c_{jl} is the eigenvector containing the expansion coefficients and the Hamiltonian h_{ij} and the overlap matrix s_{ij} are obtained via numerical integration.

$$\begin{aligned} h_{ij} &= \int d^3r [\varphi_i(\bar{\mathbf{r}}) \widehat{h}^{KS} \varphi_i(\bar{\mathbf{r}})], \\ s_{ij} &= \int d^3r [\varphi_i(\bar{\mathbf{r}}) \varphi_i(\bar{\mathbf{r}})]. \end{aligned} \tag{10}$$

Eq. (9) gives direct access to the single-particle eigenvalues [6].

The exchange-correlation functional can be broken in to exchange and correlation parts $E_{xc} = E_x + E_c$. For the local density approximation and the generalized gradient approximation calculation of the exchange correlation energy is a single integral over real space

$$E_{xc}[n] = \int d^3r f_{xc}[n(\bar{\mathbf{r}}), |\nabla n(\bar{\mathbf{r}})|^2], \tag{11}$$

where the exchange-correlation energy depends only on the density and its gradient. Such a calculation is not a very time or memory consuming operation [5, 6].

For hybrid functionals the correlation energy E_c remains the same as before but the exchange energy is substituted in part by the exact exchange

$$E_x^{Hybrid} = E_x^{GGA} - \alpha E_x^{GGA} + \alpha E_x^{HF}, \tag{12}$$

[3, 4] where α is the mixing parameter and

$$E_x^{HF} = \frac{1}{2}\sum_{kl}(ij|kl) \tag{13}$$

is the Hartee-fock exchange energy [3, 4] and

$$(ij|kl) = \int\int \frac{\psi_i^*(\overline{\mathbf{r}})\psi_j^*\psi_i^*(\overline{\mathbf{r}})\psi_k(\overline{\mathbf{r}}')\psi_l(\overline{\mathbf{r}}')}{|\overline{\mathbf{r}} - \overline{\mathbf{r}}'|} d\overline{\mathbf{r}} d\overline{\mathbf{r}}' \tag{14}$$

is the four-index Coulomb integral [3,4]. For the Heyd-Scuseria-Ernzerhof (HSE06) hybrid functional Coulomb like $\frac{1}{r}$ interaction is replaced with short-range $\mathrm{erfc}\frac{(\omega r)}{r}$ interaction where ω is the screening parameter [3]. Now the HSE06 exchange energy is given by

$$E_x^{HSE06}(\omega) = E_x^{PBE} - \alpha E_x^{PBE}(\omega) + \alpha E_x^{HF}(\omega), \tag{15}$$

where E_x^{PBE} takes care of the missing long-range exchange energy and PBE stands for the Perdew–Burke-Ernzerhof functional which embodied the GGA. For the HSE06 ω is 0.11 bohr^{-1} and in the standard case $\alpha = 0.25$.

During the s.c.f cycle iterations only the total energies and the eigenvalues are needed [5, 6]. Since the exchange–correlation energy functional which is correct for the total energy replaces the exchange–correlation potential energy which is included in the eigenvalues, this term must be deducted from the eigenvalues

$$E_{tot} = \sum_{l=1}^{N_{states}} f_l\epsilon_l - \int d^3r[n(\overline{\mathbf{r}})v_{xc}(\overline{\mathbf{r}})] + E_{xc}[n] - \frac{1}{2}\int d^3r[n(\overline{\mathbf{r}})v_{es}(\overline{\mathbf{r}})] + E_{nuc-nuc}. \tag{16}$$

In purpose of the minimum energy E_0 calculation or for the fitting of dimer-curves / calculation of the lattice-constant a_0 and for the calculation of bulk-modulus B_0 for bulk-structures the Birch –Murnaghan equation of state

$$E_{tot}(a) = E_0 + \frac{9V_0B_0}{16}\{[(\frac{a_0}{a})^2 - 1]^3B_0' + [(\frac{a_0}{a})^2 - 1]^2[6 - 4(\frac{a_0}{a})^2]\} \tag{17}$$

[2, 5] is used. Here $B_0' = (\frac{\partial B}{\partial P})_T$. For the dimer-curve fitting a can vary from the equilibrium a_0 quite a bit, but the bulk-modulus is quite sensitive quantity which is why a shouldn't vary from a_0 a lot.

2.2 NAO basis functions and auxiliary basis

The numeric atom-centered orbital (NAO) basis functions are defined as

$$\varphi_i(\bar{\mathbf{r}}) = \frac{u_i(r)}{r} Y_{lm}(\Omega), \tag{18}$$

with $Y_{lm}(\Omega)$ being the spherical harmonic and u_i is a function tabulated numerically which ensures flexibility [6]. For the construction of the NAO basis set, the Schrödinger-like radial equations

$$[-\frac{1}{2}\frac{d^2}{dr^2} + \frac{l(l+1)}{r^2} + v_i(r) + v_{cut}(r)]u_i(r) = \epsilon_i u_i(r). \tag{19}$$

are solved. Radial functions are defined by the term $v_i(r)$ which is responsible for the main behavior of the radial function and the term $v_{cut}(r)$ is known as the confining potential and it is responsible for smooth decay of the radial function [6]. The $v_{cut}(r)$ is defined as

$$v_{cut}(r) = \begin{cases} 0 & r \leq r_{onset}, \\ s \cdot \exp\left(\frac{w}{r - r_{onset}}\right) \cdot \frac{1}{(r - r_{cut})^2} & r_{onset} \leq r \leq r_{cut}, \\ \infty & r \geq r_{cut}. \end{cases} \tag{20}$$

Here s is a scaling parameter and the width $w = r_{cut} - r_{onset}$ defines how fast the confining potential increases from 0 to ∞. In practice the width is [1.5Å-2.0Å]. Radial functions are orthonormalized via use of the Gram-Schmidt process on a logaritmic radial grid.

Construction of the basis set begins with defining large pool of hydrogen-like, cation-like or atom-like functions u_i determined by the form of the potential $v_i(r)$. The hydrogen-like functions usually perform very well [6]. The first step is to construct an initial minimal free-atom basis set. Following this step the radial functions that give the largest improvement to the total energy are added one by one to the original basis set. This is done until no significant improvement is noticed in the total energy. Test of the energy convergence is done on a simple dimer for 4 to 5 different bond distances [5, 6]. Since no basis function overlap occur from other available atom centers no accidental improvement to the total energy occur. The basis functions are divided to different tiers according to how big improvement to the total energy they give. The basis size increases the accuracy of the calculation performed but is also crucial for the resources needed for the calculation (CPU-time and memory). Especially the high angular momentum functions h,g or even f-functions can increase the cost of the calculation significantly in particular when using the hybrid XC-functionals [5,6]. Because of this, hierarchy of the settings light, tight and really-tight are provided for all elements in the FHI-aims package [5, 6]. The category called intermediate sits between the light and the tight for the computational cost and accuracy/level of the convergence of the calculation [5]. The main purpose of this category is to reduce cost of the calculation using the hybrid-functionals e.g. the HSE06-functional [5].

The two electron Coulomb operator needed in the hybrid functional and Hartee-Fock calculations motivates the use of auxiliary basis functions. The auxiliary basis functions P_μ expand the pair products $\rho_{ij}(\bar{\mathbf{r}})$ of the basis functions φ_i and φ_j. They are defined as

$$\rho_{ij}(\bar{\mathbf{r}}) \equiv \varphi_i(\bar{\mathbf{r}})\varphi_j(\bar{\mathbf{r}}) \approx \tilde{\rho}_{ij}(\bar{\mathbf{r}}) \equiv \sum_{\mu}^{N_{aux}} C_{ij}^{\mu} P_\mu(\bar{\mathbf{r}}), \tag{21}$$

where C_{ij}^{μ} denotes expansion coefficients and $\tilde{\rho}_{ij}(\bar{\mathbf{r}})$ denotes the approximate expansion. Via use of the auxiliary basis, the four-center two-electron integrals can be reduced

$$\begin{aligned}(ij|kl) = \int\int \frac{\varphi_i(\bar{\mathbf{r}})\varphi_j(\bar{\mathbf{r}})\varphi_k(\bar{\mathbf{r}}')\varphi_l(\bar{\mathbf{r}}')}{|\bar{\mathbf{r}} - \bar{\mathbf{r}}'|} d\bar{\mathbf{r}} d\bar{\mathbf{r}}' \approx \sum_{\mu\nu} C_{ij}^{\mu}(\mu|\nu) C_{ij}^{\nu}, \text{ where} \\ (\mu|\nu) = V_{\mu\nu} = \int \frac{P_\mu(\bar{\mathbf{r}})P_\nu(\bar{\mathbf{r}})}{|\bar{\mathbf{r}} - \bar{\mathbf{r}}'|} d\bar{\mathbf{r}} d\bar{\mathbf{r}}'\end{aligned} \tag{22}$$

[4]. Different methods to evaluate C_{ij}^{μ}, originate from different resolution of identity (RI) methods. Most known is the RI-V but for bigger periodic bulk-structures the LVL-fast RI-method is being used [3–5]. RI-LVL retains localization of auxiliary function μ of basis function product (i, j) on atoms I and J, and for the rest of the atoms $C_{ij}^{\mu} = 0$ [3].

2.3 Integration in real and k-space

Due to the confining potential, the basis functions are non-zero only inside a fixed volume. This encourages to divide the Hamiltonian and overlap integrals over the space Eq. (10) to a sum of atom centered integrals, i.e.,

$$\int d^3r \varphi_i(\bar{\mathbf{r}}) \widehat{h}^{KS} \varphi_j(\bar{\mathbf{r}}) = \sum_{at} \int d^3r p_{at}(\bar{\mathbf{r}}) \varphi_i(\bar{\mathbf{r}}) \widehat{h}^{KS} \varphi_j(\bar{\mathbf{r}}), \tag{23}$$

where $p_{at}(\bar{\mathbf{r}}) = \frac{g_{at}(\bar{\mathbf{r}})}{\sum_{at'} g_{at'}(\bar{\mathbf{r}})}$ is the atom-centered partition function and g_{at} is a strongly peaked density-function [6]. In practice Eq. (23) can be expanded as a sum of weighted products over grid points in atom centered grids

$$\int d^3r \varphi_i(\bar{\mathbf{r}}) \widehat{h}^{KS} \varphi_j(\bar{\mathbf{r}}) = \sum_{at,s,t} w(\bar{\mathbf{r}}) \varphi_i(\bar{\mathbf{r}}) \cdot [\widehat{h}^{KS} \varphi_j(\bar{\mathbf{r}})], \tag{24}$$

where $w(\bar{\mathbf{r}})$ is the weight and summation goes over the atoms, radial shells and angular points in each shell [6].

For periodic boundary conditions, e.g. in the case of the bulk-structures the Kohn-Sham generalized eigenvalue equation Eq. (9) becomes $\bar{\mathbf{k}}$-space dependent. This motivates to define Bloch-like generalized basis functions

$$\chi_{i,k}(\bar{\mathbf{r}}) = \sum_{N} \exp[i\bar{\mathbf{k}} \cdot \bar{\mathbf{T}}(\bar{\mathbf{N}})] \cdot \varphi_i[\bar{\mathbf{r}} - \bar{\mathbf{R}}_{at} + \bar{\mathbf{T}}(\bar{\mathbf{N}})], \tag{25}$$

with $\bar{\mathbf{T}}(\bar{\mathbf{N}})$ being a translation vector of the computational unit-cell [6]. Now the Hamiltonian is expanded as a sum of

$$h_{ij}(\bar{\mathbf{k}}) = \sum_{M,N'} \exp\{i\bar{\mathbf{k}} \cdot [\bar{\mathbf{T}}(\bar{\mathbf{N}}) - \bar{\mathbf{T}}(\bar{\mathbf{M}})]\} \cdot h_{ij}^{uc}(\bar{\mathbf{N}}, \bar{\mathbf{M}}), \tag{26}$$

where $h_{ij}^{uc}(\bar{\mathbf{N}}, \bar{\mathbf{M}})$ is the Hamiltonian over a one unit cell. Here the sum over $\bar{\mathbf{M}}$ and $\bar{\mathbf{N}}$ stands for the summing over only unit cells whose basis functions $\varphi_{i,\bar{\mathbf{M}}}, \varphi_{j,\bar{\mathbf{N}}}$ differ from zero inside the first unit cell.

2.4 Self-consistency

Equations of DFT are nonlinear due to the fact that Hamiltonian operator depends on the electron density which depends on the eigenvectors. The self-consistent field (s.c.f.) method is an iterative method used to converge the density, eigenvalues and total energy. The K-S orbitals $|\psi_l^{(\mu)}\rangle$ are obtained from the Hamiltonian of the previous s.c.f. iteration $h_{ij}^{(\mu-1)}$ [6], which is based on a mixed density

$$n^{(\mu)} = n^{(\mu-1)} + \widehat{G}^1(n_{KS}^{(\mu)} - n^{(\mu-1)}), \tag{27}$$

where μ stands for a number of iteration and $\widehat{G}^1$ is a constant charge mixing parameter [5, 6]. $\widehat{G}^1$ also dampens the fluctuation of the electron density and ensures the convergence of the solution. Eq. (27) is the linear mixer.

The s.c.f cycle begins with a initial charge density guess based on the superposition of the free-atom densities

$$n^{(0)}(\bar{\mathbf{r}}) = \sum_{at} n_{at}^{free}(|\bar{\mathbf{r}} - \bar{\mathbf{R}}_{\mathbf{at}}|) \tag{28}$$

[6]. In a more complex mixing scheme called the Pulay mixer Eq. (29) the optimization of the electron density is done by minimizing residuals $R^{(\mu)} = n_{KS}^{(\mu)} - n^{(\mu-1)}$ of the N_p previous iterations.

$$n^{(\mu)} = \widehat{G}^1[R^{(\mu)} + \sum_{k=1}^{N_p} \bar{\alpha}_k(R^{(\mu-k+1)} - R^{(\mu-k)})] + n^{(\mu-1)} + \sum_{k=1}^{N_p} \bar{\alpha_{\mathbf{k}}}(n^{(\mu-k)} - n^{(\mu-k-1)}) \tag{29}$$

During the s.c.f cycle v_{es} is evaluated after mixing but from $n^{\mu-1}$ instead of n^{μ}. Re-evalution of v_{es} during same the iteration is avoided in means of use of Harris functional instead of Eq. (1)

$$\begin{aligned} E_{Harris}^{\mu} = & \sum_{l=1}^{N_{states}} f_l^{(\mu)} \epsilon_l^{(\mu)} - \int d^3r [n^{(\mu-1)}(\bar{\mathbf{r}}) v_{xc}[n^{(\mu-1)}](\bar{\mathbf{r}})] \\ & + E_{xc}[n^{(\mu-1)}] - \frac{1}{2} \int d^3 3 [n^{(\mu-1)}(\bar{\mathbf{r}}) v_{es}^{(\mu-1)}(\bar{\mathbf{r}})]. \end{aligned} \tag{30}$$

2.5 Relativity

Near the nuclei $|\epsilon - v(\bar{\mathbf{r}})| \to 2c^2$ and a need of the Dirac's four-component equation arises [6]. This is urgent especially for the heavier elements since any wave function part close to the nuclei is greatly modified. Instead of the Dirac's four-component equation choice of a one-component, scalar-relativistic scheme by neglecting the spin-orbit coupling

$$(\bar{\mathbf{p}} \cdot \frac{c^2}{2c^2 + \epsilon_l - v} \cdot \bar{\mathbf{p}} + v)\psi_l = \epsilon_l \psi_l \tag{31}$$

is employed. This choice preserves the computational cost of the Schrödinger-like equation [6]. The scaled zeroth order regular approximation (ZORA) is used for a scalar-relativistic kinetic energy operator

$$\widehat{t}_{ZORA} = \bar{\mathbf{p}} \cdot \frac{c^2}{2c^2 - v} \cdot \bar{\mathbf{p}}. \tag{32}$$

Replacement of v with $v_{at(j)}^{free}$ in Eq. (32) results in an approximation

$$\widehat{t}_{ZORA}|\varphi_j\rangle = \bar{\mathbf{p}} \cdot \frac{c^2}{2c^2 - v_{at(j)}^{free}} \cdot \bar{\mathbf{p}}|\varphi_j\rangle, \tag{33}$$

known as the atomic ZORA [5,6]. Due to the index j referring to the basis function φ_j symmetrization is in order and is done via the use of

$$T_{ij} = \frac{1}{2}(\langle\varphi_i|\widehat{t}_{ZORA}|\varphi_j\rangle + \langle\varphi_j|\widehat{t}_{ZORA}|\varphi_i\rangle). \tag{34}$$

2.6 Spin

In a spin-polarized calculation there are two spin densities $n^{\uparrow}$ and $n^{\downarrow}$. Total electron density calculated via Eq. (3) is now modified

$$n(\bar{\mathbf{r}}) = n^{\uparrow}(\bar{\mathbf{r}}) + n^{\downarrow}(\bar{\mathbf{r}}) = \sum_{n\sigma}^{occ} f_l |\psi_{n\sigma}(\bar{\mathbf{r}})|^2, \tag{35}$$

where σ denotes spin indexes $\uparrow$ and $\downarrow$ [4]. In a spin polarized calculation rest of the terms in Eq. (1) correspond to the total electron density n except the exchange-correlation term E_{xc} that corresponds to n^{σ}. This results in the spin-dependent Hamiltonian $H(n^{\sigma})$. Due to this during the s.c.f cycle we now have two eigenvalue problems to solve instead of one resulting in increased use of resources [5].

3 Simulations

3.1 differences between hierarchy classes

As mentioned earlier FHI-aims provides four different settings: light, intermediate, tight and really-tight [5,6]. During the search of the intermediate settings the focus is on the differences between the light and the tight settings. The differences can be in the number of basis functions or in the density of the integration grid. The differences are in the basis functions due to the tight class embodying more basis functions and due to v_{cut} having bigger r_{onset} and width w but the same scaling parameter s see Eq. (20). Due to these differences also the integration grid of tight settings needs to be denser in order to avoid under-integration.

The intermediate settings embody the same integration grid as the tight settings. The difference between these two settings is mostly due to the set of basis functions used. Some of the basis functions of the tight class are either dropped or modified to auxiliary basis functions [5]. In the case of a big difference between the confining potential v_{cut} parameters between the light and the tight category, the intermediate category can embody parameters between these categories. Otherwise the confining potential of the intermediate category is equivalent to that of the tight category [5].

General differences between the light- and the tight-settings are tight having at most 434 angular integration points per radial integration shell instead of at most 302 points for light. The tight-settings also have two times more shells than the light-settings and outermost shell of the tight-settings is 7 Å away from the atom in discussion instead of 5.5 Å for the light-settings. Also while calculating the Hartee potential Eq. (7) cutoff parameter l^{es}_{max} is 6 for the tight-settings and 4 for the light-settings.

Since the oxide calculations are performed for all of the elements considered in this work differences between the intermediate- and the tight-settings of oxide have an impact on the results. The pool of the basis functions differs quite a bit between the tight- and the intermediate-settings. For the intermediate-settings hydrogen-like 4f basis function is an auxiliary basis function unlike for the tight-settings. For the intermediate-settings also hydrogen-like basis functions 3p, 3d and 1s are ignored (here first number stands for the principal quantum number and the letter stands for the orbital quantum number). Confining potentials for the tight- and the intermediate settings are the same cut-pot$_{tight}$=[4.0, 2.0, 1.0]Å. Here the first parameter is the r_{onset} and the second one is w and the third one is scaling parameter s.

3.2 Structures used for simulations

The simulations where done for five different chemical environments (free-atom, dimer, cluster of 6 atoms, bulk and oxide) and for the sodium also for the hydroxide-molecule. Of these simulated cases the bulk and the oxide cases were periodic structures. Table 1 lists the periodic structures used for the simulations. For

reference these structures had already been used for simulations and were found from [7].

Notice that the bcc-unit (body-centered cubic unit-cell) and bcc-conv (body-centered cubic conventional-cell) are the same structure, but bcc-conv contains twice as many lattice-points and that $a_{bcc-conv}=2\times a_{bcc-unit}$.

case & atom	structure	lattice-points	lattice-vectors	k-grid
bulk, Na	bcc-unit	Na[0,0,0]	[-a,a,a], [a,-a,a], [a,a,-a]	[24×24×24]
bulk, K, Mn Mo, Cr	bcc-conv	K[0,0,0], K[c,c,c]	[a,0,0], [0,a,0], [0,0,a]	[24×24×24] [20×20×20]
bulk, Pt	fcc	Pt[0,0,0], Pt[c,c,0] Pt[c,0,c], Pt[0,c,c]	[a,0,0], [0,a,0], [0,0,a]	[16×16×16]
oxide, Na	fcc	O[0,0,0], O[c,c,0] O[c,0,c]O[0,c,c] Na[b,b,b] ,Na[d,b,b] Na[b,d,b], Na[b,b,d] Na[d,d,b], Na[d,b,d] Na[b,d,d], Na[d,d,d]	[a,0,0], [0,a,0], [0,0,a]	[12×12×12]
oxide, K	fcc	O[0,0,0], K[b,b,b] K[d,d,d]	[c,c,0], [c,0,c], [0,c,c]	[24×24×24]
oxide, Pt, Mo, Mn Cr	bcc	Pt[0,0,0] Pt[c,c,c] O[c,c,0], O[c,0,c] O[0,c,c]	[a,0,0], [0,a,0], [0,0,a]	[16×16×16] [12×12×12]

Table 1: Periodic structures used for simulations. Here b=0.25×a, c=0.5×a, d=0.75×a. Here K, Mn, Mo and Cr use the same structure for bulk-calculations but K and Mn use [24×24×24] k-grid and Mo and Cr use [20×20×20] k-grid. Similarly in oxide calculations for Pt, Mo, Mn and Cr the k-grid used for Pt, Mo and Mn is [16×16×16] and the k-grid used for Cr is [12×12×12].

3.3 Sodium

The differences between the tight- and the light-settings of sodium are mostly due to the used set of the basis functions u_i. The tight-settings embodies all of the basis functions of the light-settings (minimal + tier1), but also embodies all four of the tier2 basis functions u_i, i.e., hydrogen 4p, hydrogen 3s, hydrogen 4f and hydrogen 4d basis functions. Here hydrogen stands for hydrogen-like basis-functions, first number stands for the principal quantum number and the letter stands for the orbital quantum number.

The scaling parameter s of confining potential v_{cut} for is 1 for both the light- and the tight-settings and for rest of the atoms of this work also Sections 3.4 to 3.8. The confining potential differs with the tight-setting having $r_{onset} = 5.0$Å and $w = 2.0$Å instead of the light-setting counterparts $r_{onset} = 4.0$Å and $w = 1.5$Å. Search of the intermediate settings is done via use of two different confining potentials v_{cut}, with $r_{onset} = 5.0$Å and $w = 2.0$Å and $r_{onset} = 4.5$Å and $w = 2.0$Å. The set of basis functions varies from light-basis + 4f hydrogen via auxiliary basis, light + hydrogen 4p + hydrogen 3s and hydrogen 4f via auxiliary basis, light + hydrogen 4p and hydrogen 3s, light + hydrogen 4p, hydrogen 3s + hydrogen 4d. Since LDA doesn't use auxiliary basis functions, the use of the auxiliary hydrogen-like 4f basis function means that for the LDA calculations hydrogen-like 4f basis function is ignored. This feature follows for the rest of the LDA calculations present in this paper in Sections 3.4 to 3.8.

In Tables 2 and 3 cut-pot$_1$=[4.5, 2.0, 1.0] Å and for the rest of the intermediate-settings candidates cut-pot$_{tight}$=[5.0, 2.0, 1.0] was being used. The crystal structure of the bulk-simulation was the body-centered cubic (see Table 1) and the results are shown in Table 2.

basis and cut-pot	E0 [eV]	V0 [Å^3]	a0 [Å]	B0 [eV/Å^3]
LDA				
light	-4400.3116	33.407	2.02889	0.05781
tier1+aux 4f	-4400.3142	33.489	2.03055	0.05684
tier1+4p+3s+aux 4f cut-pot$_1$	-4400.3194	33.203	2.02475	0.05622
tier1+4p+3s+aux 4f	-4400.3204	33.155	2.02378	0.05705
tight	-4400.3226	33.235	2.02540	0.05662
HSE06				
light	-4414.6406	38.117	2.12008	0.04664
tier1+aux 4f	-4414.6469	38.484	2.12687	0.04715
tier1+4p+3s+aux 4f cut-pot$_1$	-4414.6592	37.857	2.11524	0.04690
tier1+4p+3s+aux 4f	-4414.6601	37.844	2.11501	0.04641
tight	-4414.6667	37.950	2.11698	0.04775

Table 2: Sodium bulk-simulation.

The crystal structure of oxide-simulation was fcc (see Table 1). Structure embodied four oxide-atoms and eight sodium atoms. Table 3 contains results of the sodium oxide-simulation.

Hydroxide simulation was a non-periodic cluster simulation with one Na-atom, one O-atom and one H-atom. System was relaxed before the final total energy calculation. Table 4 contains results of the sodium hydroxide molecule-simulation.

Simulations were also conducted on a free-atom system with and without spin polarization, on a Na-dimer and on a cluster with six Na-atoms. Noteworthy about these simulations is that every intermediate settings candidate performed well with non periodic systems, but only few performed well the on bulk and oxide calculations especially with the HSE06 functional.

basis and cut-pot	E0 [eV]	V0 [Å^3]	a0 [Å]	B0 [eV/Å^3]
LDA				
light	-43352.5889	158.396	5.41063	0.36360
tier1+aux 4f	-43352.6103	158.522	5.41207	0.35797
tier1+4p+3s+aux 4f cut-pot$_1$	-43352.6864	158.224	5.40868	0.35937
tier1+4p+3s+aux 4f	-43352.6838	158.194	5.40833	0.35920
tight	-43352.8544	157.942	5.40546	0.35850
HSE06				
light	-43592.0278	167.863	5.51635	0.32126
tier1+aux 4f	-43592.0627	168.054	5.51844	0.32251
tier1+4p+3s+aux 4f cut-pot$_1$	-43592.2064	167.585	5.51330	0.32581
tier1+4p+3s+aux 4f	-43592.2098	167.569	5.51312	0.32568
tight	-43592.3790	167.324	5.51043	0.30410

Table 3: Sodium oxide-simulation.

XC	basis and cut-pot	E0 [eV]
LDA	light	-6454.6972
LDA	tier1+4f-aux	-6454.8273
LDA	tier1+4p+3s+aux 4f cut-pot$_1$	-6454.8326
LDA	tier1+4p+3s+aux 4f	-6454.8335
LDA	tight	-6454.8435
HSE06	light	-6488.0562
HSE06	tier1+4f-aux	-6488.1584
HSE06	tier1+4p+3s+aux 4f cut-pot$_1$	-6488.1675
HSE06	tier1+4p+3s+aux 4f	-6488.1678
HSE06	tight	-6488.1777

Table 4: Sodium-hydroxide-molecule simulation.

Since the hydrogen-like 4f-basis can have a significant impact on the chemical bonding, we chose not to ignore it, but add it via use of the auxiliary basis. The total energies of the bulk- and the oxide-simulations without the 4p and the 3s basis function were closer to the light-settings than the tight-settings which is undesirable for the intermediate-settings. This is why choice of the intermediate-settings basis function pool of tier1+4p+3s+aux 4f was made. Change of cut-pot$_{tight}$=[5.0, 2.0, 1.0] to cut-pot$_1$=[4.5, 2.0, 1.0] didn't have a significant effect on the results, hence choice of tier1+4p+3s+aux 4f cut-pot$_1$ to be the intermediate-settings was made.

3.4 Potassium

The differences between tight- and light-settings are mostly due to the confining potential v_{cut}, cut-pot$_{tight}$= [6.0 2.0 1.0],cut-pot$_{light}$= [4.0 1.5 1.0]. Three different confining potential parameters were tested cut-pot$_1$= [4.5 2.0 1.0] ,cut-pot$_2$= [5.0 2.0 1.0], cut-pot$_3$= [5.5 2.0 1.0]. The set of basis functions varied by only the hydrogen-like 4f function which motivates to test use of auxiliary hydrogen-like 4f function in the intermediate settings.

XC	basis and cut-pot	E0 [eV]	a0 [Å]
LDA	light	-32752.7662	3.73932
LDA	tight 4f-aux cut-pot$_2$	-32753.0784	3.81370
LDA	tight cut-pot$_2$	-32753.0008	3.79637
LDA	tight	-32753.1292	3.82533
HSE06	light	-32641.4270	3.91872
HSE06	tight- 4f-aux cut-pot$_2$	-32641.7906	3.98016
HSE06	tight cut-pot$_2$	-32641.7908	3.97982
HSE06	tight	-32641.8534	4.00010

Table 5: Potassium dimer-simulation

Table 5 contains results of the potassium dimer-simulation. Bulk simulation is conducted on a body-centered cubic structure which embodies two potassium-atoms (see Table 1). Table 6 contains results of the potassium bulk-simulation.

basis and cut-pot	E0 [eV]	V0 [Å^3]	a0 [Å]	B0 [eV/Å^3]
LDA				
light	-32754.4604	120.216	4.93537	0.06289
tight 4f-aux cut-pot$_2$	-32754.4902	128.591	5.04743	0.02831
tight cut-pot$_2$	-32754.4924	128.382	5.04469	0.02847
tight	-32754.4957	128.270	5.04323	0.02724
HSE06				
light	-32841.2468	157.474	5.40012	0.06337
tight 4f-aux-cut-pot$_2$	-32841.2416	151.451	5.33037	0.02168
tight cut-pot$_2$	-32841.2434	151.074	5.32595	0.02164
tight	-32841.2492	150.897	5.32386	0.02186

Table 6: Potassium bulk-simulation

basis and cut-pot	E0 [eV]	V0 [Å^3]	a0 [Å]	B0 [eV/Å^3]
LDA				
light	-34792.3415	59.627	6.20158	0.23255
tight 4f-aux-cut-pot$_2$	-34792.4054	59.904	6.21116	0.23409
tight-cut-pot$_2$	-34792.4563	59.077	6.18242	0.24193
tight	-34792.4695	59.240	6.18812	0.23543
HSE06				
light	-34890.8656	66.028	6.41599	0.16658
tight 4f-aux-cut-pot$_2$	-34890.8792	65.506	6.39901	0.19851
tight 4f-aux-cut-pot$_3$	-34890.8855	65.583	6.40152	0.19839
tight-cut-pot$_2$	-34890.9540	65.092	6.38551	0.19964
tight	-34890.9721	65.379	6.39487	0.19304

Table 7: Potassium oxide-simulation

Oxide simulation is conducted on a face-centered cubic structure which embodies one potassium-atom and two oxide-atoms(see Table 1). Table 7 contains results of the potassium oxide-simulation. For the oxide-calculation use of auxiliary 4f basis function resulted loose of the level of convergence with use of cut-pot$_2$ and cut-pot$_3$ (see Table 7). And with use of normal 4f basis the total energy converged well. Normal 4f basis function is elected for the intermediate category instead of auxiliary 4f basis function.

For the free atom- and the cluster of six K-atoms simulations tight cut-pot$_2$ performed extremely well.

Due to cut-pot$_2$ outperforming cut-pot$_1$ by a mile and use of cut-pot$_3$ not resulting in significant improvement to the level of convergence compared to cut-pot$_2$ even though requiring more computational resources the choice of cut-pot$_2$ as v_{cut} was reasonable for the intermediate-settings. tight-cut-pot$_2$ was chosen to be the new intermediate-settings.

3.5 Platinum

The pool of basis function for the tight- and the light-settings differs by the hydrogen-like 5g basis function which is embodied by the tight-settings. The confining potentials v_{cut}, cut-pot$_{tight}$= [4.0 2.0 1.0],cut-pot$_{light}$= [3.5 1.5 1.0] are close to each other and shouldn't be touched. Search of the intermediate settings is done via use of auxiliary hydrogen-like 5g basis function. As mentioned in Section 3.3 for the LDA calculation use of auxiliary hydrogen-like 5g is being ignored and improvements for LDA calculations are due to tighter integration grid as is the case also for Sections 3.6 to 3.8.

Bulk simulation is done on face-centered cubic conventional cell which embodies four platinum-atoms (see Table 1). Table 8 contains results of the platinum bulk-simulation.

basis and cut-pot	E0 [eV]	V0 [Å^3]	a0 [Å]	B0 [eV/Å^3]
LDA				
light	-2071916.6090	59.284	3.89924	1.86869
tight-5g-aux	-2071916.8175	59.242	3.89832	1.87875
tight	-2071916.9364	59.112	3.89545	1.88701
HSE06				
light	-2073130.9312	61.694	3.95137	1.61092
tight-5g-aux	-2073136.8778	61.629	3.94998	1.61866
tight	-2073136.9915	61.490	3.94701	1.62812

Table 8: Platinum bulk-simulation

Oxide calculation is done on body-centered cubic conventional cell which embodies two Pt-atoms and and three O-atoms (see Table 1). Table 9 contains results of the platinum oxide-simulation.

basis and cut-pot	E0 [eV]	V0 [Å^3]	a0 [Å]	B0 [eV/Å^3]
LDA				
light	-1042057.947	58.364	3.87896	1.26847
tight-5g-aux	-1042058.200	58.065	3.87232	1.29351
tight	-1042058.393	57.857	3.86770	1.28794
HSE06				
light	-1042700.466	59.468	3.90326	1.22091
tight-5g-aux	-1042703.620	59.153	3.89636	1.23533
tight	-1042703.834	58.944	3.89177	1.26824

Table 9: Platinum oxide-simulation

Cluster simulation is done via relaxing the cluster of six platinum atom and calculating ground state energy of the relaxed structure. Table 10 contains results of the platinum cluster-simulation.

XC	basis and cut-pot	E0 [eV]
LDA	light	-171789.9262
LDA	5g-aux	-171790.2789
LDA	tight	-171790.4669
HSE06	light	-172115.6163
HSE06	5g-aux	-172115.9913
HSE06	tight	-172116.3812

Table 10: Platinum cluster-simulation

Tight-5g-aux did also work fine with the free-atom simulation and the dimer simulation as seen from Fig. 1. Especially for the HSE06 dimer-calculation the intermediate-settings candidate outperforms light-settings by a mile, but also for the LDA calculations notable improvement is noticed in Fig. 1. Worth of mentioning is that for repulsion-regime (smaller dimer distances than a_0) the error of the total energy increases significantly for the LDA calculations. Also since there are no other significant modifications to be made the tight-5g-aux with cut-pot$_{tight}$ remains the choice of the intermediate-settings.

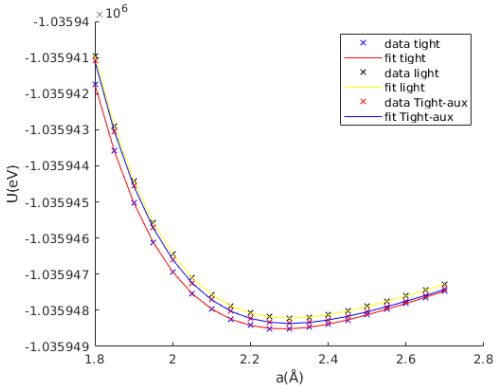

(a) Platinum LDA dimer curves

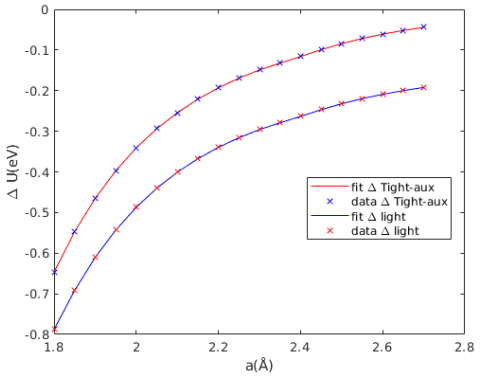

(b) Platinum LDA total energy differences compared to the tight-settings

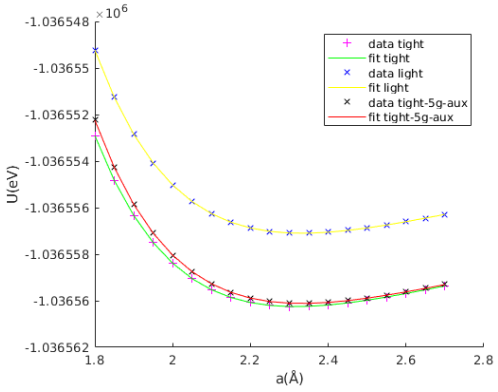

(c) Platinum HSE06 dimer curves

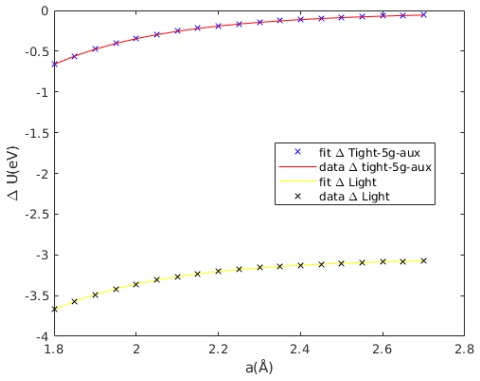

(d) Platinum HSE06 total energy differences compared to the tight-settings

Figure 1: Platinum dimer-curves

3.6 Molybdenum

Molybdenum follows the same steps as the platinum did. Once again the set of basis functions differs only by the hydrogen-like 5g basis function which is embodied by the tight-settings. The confining potentials v_{cut} are cut-pot$_{tight}$= [4.0 2.0 1.0], cut-pot$_{light}$= [3.5 1.5 1.0] and will not be touched. Search of the intermediate settings is done via use of an auxiliary hydrogen-like 5g basis function.

Bulk simulation was conducted on similar body-centered cubic cell as the potassium bulk simulation was (see Table 1). Table 11 contains results of the molybdenum bulk-simulation. The total energy of the tight-5g-aux converged well, but the lattice vector $a0$ is overestimated with tight-5g-aux settings for both the LDA and the HSE06 calculations. Nevertheless $a0$ sits still between results obtained with the tight- and the light-settings.

accuracy	E0 [eV]	V0 [Å^3]	a0 [Å]	B0 [eV/Å^3]
LDA				
light	-222238.7040	30.211	3.11450	1.75773
tight-5g-aux	-222238.7711	30.207	3.11438	1.76028
tight	-222238.8045	30.169	3.11306	1.76176
HSE06				
light	-222472.7998	31.197	3.14803	1.73081
tight-5g-aux	-222472.9330	31.195	3.14794	1.73791
tight	-222472.9670	31.086	3.14429	1.74227

Table 11: Molybdenum bulk-simulation

The oxide simulation is conducted on similar body-centered cubic cell as platinum oxide simulation(see Table 1). Table 12 contains results of the molybdenum oxide-simulation. For LDA oxide simulations tight-5g-aux sits in the middle between the light- and the tight-settings for all of the results of the Murnaghan-fit. For HSE06 the tight-5g-aux outperforms the light-settings by a mile.

accuracy	E0 [eV]	V0 [Å^3]	a0 [Å]	B0 [eV/Å^3]
LDA				
light	-228344.7982	55.952	3.82477	1.57245
tight-5g-aux	-228344.9962	55.831	3.82202	1.58327
tight	-228345.1813	55.734	3.81980	1.58882
HSE06				
light	-228614.6389	57.255	3.85423	2.06361
tight-5g-aux	-228615.0597	58.734	3.88714	2.56120
tight	-228615.2417	58.681	3.88597	2.53789

Table 12: Molybdenum oxide-simulation

Essentially for all the cases simulated (free-atom, dimer, cluster, bulk and oxide) the total energy of the tight-5g-aux settings is always closer to the total energy of the tight-settings than to the total energy of the light-settings. It is reasonable to choose the tight-5g-aux to be the intermediate settings.

3.7 Manganese

Manganese follows the same steps is search for the intermediate-settings as the platinum and the molybdenum did. The confining potentials v_{cut}, cut-pot$_{tight}$= [4.0 2.0 1.0],cut-pot$_{light}$= [3.5 1.5 1.0] are close to each other and will not be touched. Since the set of the basis functions differs once again by hydrogen-like 5g, use of auxiliary hydrogen-like 5g basis function is best guess for intermediate settings. Bulk simulation is done on similar body-centered cubic cell as the potassium- and molybdenum bulk simulations were done (see Table 1).

accuracy	E0 [eV]	V0 [Å^3]	a0 [Å]	B0 [eV/Å^3]
LDA				
light	-63164.6341	20.170	2.72210	1.97605
tight-5g-aux	-63164.6418	20.008	2.71478	2.00970
tight	-63164.6603	20.076	2.71786	1.98840
HSE06				
light	-63276.8400	20.847	2.75221	1.77521
tight-5g-aux	-63276.8460	20.824	2.75120	1.78517
tight	-63276.8603	20.807	2.75043	1.78714

Table 13: Manganese bulk-simulation

Table 13 contains results of the manganese bulk-simulation. Results the bulk calculations performed via use of the tight-5g-aux are closer to the ones with light-settings than the ones with tight-settings for both LDA and HSE06 Table 13. Nevertheless tight-5g-aux still outperforms light-settings Table 13. The oxide simulation is conducted using a similar body-centered cubic cell as in platinum- and molybdenum oxide simulations Table 1.

Table 14 contains results of the manganese oxide-simulation. Unlike for the bulk-simulations, now for the oxide simulations the results of the tight-5g-aux simulations are closer to the ones performed via use of the tight-settings than the ones performed via use of the light-settings Table 14.

accuracy	E0 [eV]	V0 [Å^3]	a0 [Å]	B0 [eV/Å^3]
LDA				
light	-69270.5048	44.677	3.54836	1.59112
tight-5g-aux	-69270.7226	44.519	3.54417	1.63863
tight	-69270.7574	44.423	3.54162	1.64037
HSE06				
light	-69419.1568	46.893	3.60609	1.46384
tight-5g-aux	-69419.2704	46.788	3.60339	1.49879
tight	-69419.3817	46.781	3.60321	1.48773

Table 14: Manganese oxide-simulation

Overall accuracy of tight-5g-aux varies quite a bit for the different simulation cases. For the LDA dimer simulation the total energy of the tight-5g-aux is closer to the total energy of the light settings than the tight settings. Also for the HSE06 free atom simulation the total energy of tight-5g-aux simulation was initially even worse than the light one, but this was due to the fact that tight-5g-aux simulation found local minimum instead of global minimum and this was fixed via applying a small external electrostatic field for the first 20 s.c.f. iterations.

Nevertheless since the tight-5g-aux performed well for the periodic simulations (bulk and oxide) and for the cluster simulations where there are more atoms which results more products between basis function so the use of auxiliary basis could have significant effect on the accuracy of the simulation, it is reasonable to set the tight-5g-aux as the intermediate settings.

3.8 Chromium

Chromium follows the same steps in search for the intermediate-settings as the platinum, the molybdenum and the manganese did but with one twist, for chromium a spin-polarized treatment must be used. In the spin-polarized simulations some of the atoms are given initial spin-moment or the total initial spin-moment is spread evenly across the whole system and the simulations are either conducted via use of fixed/restricted total spin-moment or via use the free total spin-moment.

Usually simulations for the different simulation cases of chromium (free-atom, dimer, cluster, bulk and oxide) are first done via using different initial spin-moments for the cheapest settings of the calculation (LDA-light) in order to find the spin-moment of the ground-state for the system under consideration.

accuracy	E0 [eV]	V0 [Å^3]	a0 [Å]	B0 [eV/Å^3]
LDA				
light	-57269.9791	21.704	2.78943	1.86741
tight-5g-aux	-57269.9951	21.714	2.78983	1.86552
tight	-57270.0095	21.696	2.78906	1.86726
HSE06				
light	-57377.8548	22.333	2.81609	1.84425
tight-5g-aux	-57377.8763	22.323	2.81568	1.84114
tight	-57377.8903	22.305	2.81495	1.84370

Table 15: Chromium bulk-simulation

The bulk simulation is done using a similar body-centered cubic cell as the potassium, molybdenum and manganese bulk simulations (see Table 1). For the bulk simulation spin-moment 0 minimized the total energy. This means bulk simulations can be conducted via ignoring effect of spin and saving some computational resources (see Section 2.6). Table 15 contains results of the chromium bulk-simulation and in Section 3.8 these results are fitted via use of the Eq. (17).

The results of the tight-5g-aux bulk-calculations were closer to the ones performed via use of the tight-settings than the ones performed via use of the light-settings as desired. Worth of mentioning is that for repulsion-regime the error of the total energy increases significantly for both the HSE06 and the LDA calculations.

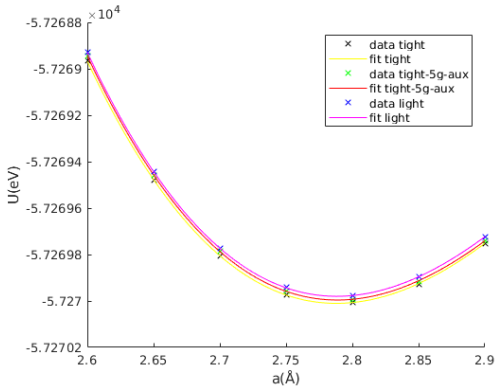

(a) Chromium LDA Murn-fits

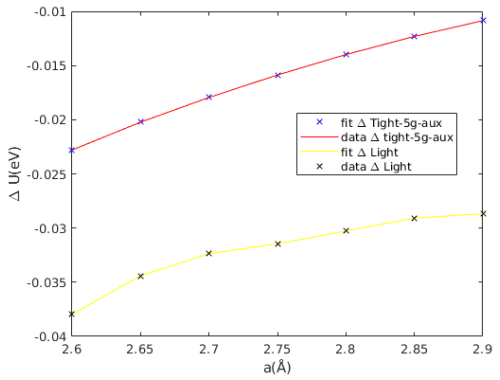

(b) Chromium LDA Murn-fit total energy differences compared to the tight-setting

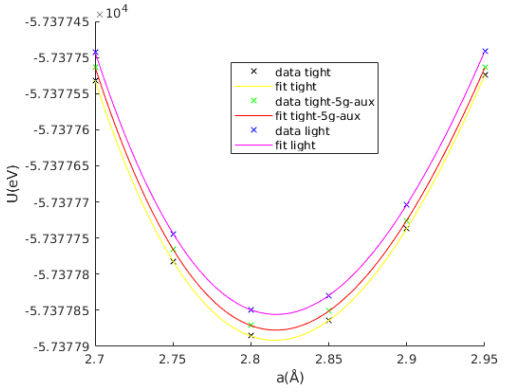

(c) Chromium HSE06 Murn-fits

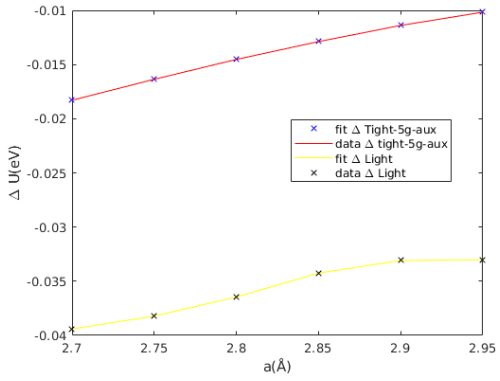

(d) Chromium HSE06 Murn-fit total energy differences compared to the tight-setting

Figure 2: Chromium bulk Murn-fits

The oxide simulation is conducted on a similar body-centered cubic unit cell as platinum, molybdenum and manganese oxide simulations were conducted (see Table 1). For the oxide simulations the initial spin-moments were given for the two chromium-atoms instead any of the three oxide-atoms in the unit cell under discussion. The final spin-moment 5 minimized the total energy of the system. Worth of mentioning is that the total energy of the spin-moment 4 simulation was very close to the total energy of the spin-moment 5 simulation. In the oxide simulations the results of the tight-5g-aux simulations are between the ones performed via use of the tight-settings than the ones performed via use of the light-settings (see Table 16).

accuracy	E0 [eV]	V0 [Å^3]	a0 [Å]	B0 [eV/Å^3]
LDA				
light	-63379.0646	47.751	3.62793	1.50783
tight-5g-aux	-63379.1774	47.683	3.62622	1.53630
tight	-63379.2917	47.629	3.62486	1.53863
HSE06				
light	-63524.9824	49.406	3.66938	1.42390
tight-5g-aux	-63525.1019	49.303	3.66683	1.41669
tight	-63525.2279	49.251	3.66554	1.41724

Table 16: Chromium oxide-simulation

For the cluster case spin-moment 2 minimized total energy. It needs to be mentioned that the final spin-moment for cluster simulations with prerelaxed geometries with use of high initial spin-moments tend to fall to local minimum 4 instead of the global minimum 2. Convergence of HSE06 cluster calculations was also extremely hard to achieve and due to this tighter integration grid and extremely low charge-mixing parameter were used Eqs. (27) and (29). The intermediate candidate (tight-5g-aux) performed well in the cluster calculations for both LDA and HSE06 calculations.

For the dimer simulation spin-moment 0 minimized the total energy. The total energy of the intermediate-settings candidate (tight-5g-aux) was between the light- and the tight-settings, but also closer to the light-settings. For the free-atom simulation the increase of the used spin-moment reduced the total energy. The maximum allowed spin-moment was 6 and it was used for the free-atom calculations.

The total energy of the tight-5g-aux settings for all the cases simulated always sat between the total energy of the tight-settings and the total energy of the light-settings. It is reasonable to choose the tight-5g-aux to be the intermediate settings.

3.9 Savings in computational resources

Atom	Δt_{iter} %	Δmemory %
bulk		
Na	-70.6	-52.8
K	-0.15	-0.51
Pt	-28.0	-17.6
Mo	-32.9	-20.4
Mn	-36.8	-24.4
Cr	-36.1	-24.6
oxide		
Na	-78.6	-62.1
K	-33.8	-32.3
Pt	-41.3	-25.3
Mo	-44.1	-36.3
Mn	-59.3	-43.6
Cr	-60.3	-44.2

Table 17: Computational resources saved in the HSE06 bulk- and oxide-simulations

Table 17 displays relative savings in computational resources for HSE06 bulk calculation when using the chosen intermediate-settings (see Sections 3.3 to 3.8) versus the tight-settings for the same calculation. Δt_{iter}% is the average relative savings in time for one s.c.f. iteration and Δmemory % is the savings in average memory usage during the iteration. The choice of representing the relative savings instead of the actual savings was done due to the fact that resource usage varied for different atoms quite a bit e.g. savings of the actual memory usage for the platinum bulk was around 31 Gb and for the sodium bulk around 58 Gb. Same goes with the actual t_{iter} e.g. for sodium the average time saved per iteration was around 220 s and for platinum the average time saved per iteration was around 900 s with use of 24 CPUs. In HSE06 calculations around 99 % of the time goes to the Fock matrix evaluation. For periodic HSE06 calculations also time to calculate the Coulomb matrices before the start of s.c.f. cycle is significant e.g. around 9500 s for platinum with tight-settings and 24 CPUs.

The difference between the computational resources required was the most prominent for the sodium calculation. This is due to a few factors. Firstly sodium was the only atom, for which a basis function (hydrogen-like 4d) function was dropped, also it was the smallest atom so that the basis function pool was originally smallest and dropping one basis function and using an auxiliary function (hydrogen-like 4f) had a significant effect on the whole set of basis functions and hence on the required computational resources. The adjustment of r_{onset} paramenter of v_{cut} had some effect. Result of the adjustment of r_{onset} paramenter of v_{cut} can be seen also from the results of potassium calculation for whom the pool of basis functions was untouched and only adjustment to the intermediate-settings

compared to the tight-settings was made to r_{onset} parameter. The savings in resources due to adjustment of r_{onset} were minimal (see Table 17) Potassium and sodium are the only ones with adjustment of v_{cut}.

For rest of the atoms (Pt, Mo, Mn and Cr) same steps to creating intermediate-settings were taken, use of auxiliary function for hydrogen-like 5g (see Sections 3.5 to 3.8). Decrease of the computational resources employed now follows closely to the atomic number atoms. Cr (z=24) and Mn (z=25) are the the smallest atoms, and decrease of the computational resources employed for the bulk-calculations were the most significant and very similar since the basis sets for Cr and Mn are very similar size. Since molybdenum (z=42) is bigger than Cr or Mn, the relative decrease of the computational recourses employed was smaller. The relative decrease of the computational recourses employed by Mo-bulk calculation was still bigger than for the biggest atom platinum (z=78) studied in this work with the same treatment for intermediate settings.

Savings in computational resources for the oxide calculations were similar as in for the bulk calculations as seen from Table 17 but with even more savings in the computational resources due to the major differences between the set of basis functions for the tight- and the intermediate-settings of oxide (see Section 3.1). The ratio between the oxide atoms compared to the atoms of elements under discussion for the sodium-oxide and the potassium-oxide cells was (1:2) (see Table 1) was less compared to oxide cells of Pt-, Mo-, Mn- and Cr-oxides (3:2) (see Table 1) and hence the savings in resources for the oxide-calculations compared to the bulk-calculations didn't increase as much for sodium and potassium as it did for Pt, Mo, Mn and Cr.

4 Conclusions

In this work DFT-calculations performed via use of the numerically tabulated atom-centered orbitals (NAOs) were considered. The focus was on finding a balance between the level of accuracy and the use of the computational resources. This was done via producing the new settings for the calculations called the intermediate settings. The accuracy and the computational resources required for the calculations via use of the intermediate-settings were between the predetermined settings called light and tight. This topic is important while working with the hybrid exchange–correlation functionals especially for bigger periodic systems. For this work the hybrid functional under the scope was the HSE06 but the effect of the use of the intermediate settings should be similar for all hybrid functionals.

The intermediate settings were produced for six different elements (Na, K, Pt, Mo, Mn and Cr). The level of accuracy of these new intermediate settings were verified on five different chemical environments (free-atom, dimer, cluster of six atoms under the discussion, bulk and oxide) and for sodium also on a hydroxide-molecule.

Three different methods were used while producing the new intermediate settings. The first method was decreasing the pool of basis functions. This method was only used for sodium. For sodium the exclusion of the hydrogen-like 4d basis-function was acceptable without loosing too much accuracy, but exclusion of hydrogen-like 4s/3d basis-functions resulted too big variations for the total energy and distances between atoms especially for periodic structures (see Tables 2 and 3).

The second method was adjustment of r_{onset} parameter of v_{cut}. This method decreases of the radius of the non-zero basis functions and hence the computational effort needed for performing the calculation. This method was exploited for the two alkali metal (Na and K), for whom r_{onset} parameter differs significantly between the tight- and the light-settings and allows flexibility to adjust r_{onset} parameter for the intermediate-settings.

The third method was the use of auxiliary basis functions instead of normal basis functions. This method can be used for the hybrid-functional calculations where calculation of the Hartee-Fock exchange energy requires calculation of the four-index Coulomb integral. This method was used for the highest angular-momentum basis function for all of the atoms under discussion except potassium while producing the intermediate settings (hydrogen-like 4f functions for Na and hydrogen-like 5g functions for Pt, Mo, Mn and Cr). For HSE06 calculation this method retains most of physical behavior of the original high angular-momentum basis function but decreases the computational resources required for calculation especially for bigger periodic systems. For the LDA calculations the auxiliary basis function is ignored.

The savings on computational resource by using the intermediate-settings instead of the tight-settings is discussed in Section 3.9. The relative savings in computational resources for the bulk and the oxide calculations were listed in Table 17. The order of magnitude of the savings in resources by elements was learned to be similar for both the bulk- and the oxide-calculations. For the oxide-calculations the ratio between the oxide-atoms versus the atoms of the element under discussion in the cell had significant influence on the savings in resources. Due to the large differences between the intermediate and tight settings for oxygen the higher ratio of oxide-atoms versus the atoms of element under discussion resulted the higher relative savings in computational resources of the oxide-calculation versus the bulk-calculation of same element.

What was learned is that the use of the intermediate-settings for sodium had biggest impact on the savings in the computational resources, due to the fact that sodium was the only atom for which the earlier discussed method of decreasing the pool of the basis functions could be employed. Sodium and potassium were the only two atoms for which r_{onset} parameter was being adjusted. The use of an auxiliary basis function instead of a normal basis function was exploited by all of the atoms under discussion of this paper except for potassium for whom the use of an auxiliary 4f basis function resulted ill behavior for the oxide-calculation. For atoms with bigger atomic number z, the pool of basis function is bigger and hence the similar adjustment to the set of basis functions has smaller effect on the computational cost of the calculation. This was seen by the fact that for Pt, Mo, Mn and Cr the procedure of formating the intermediate-settings followed exactly the same steps, but for platinum the use of the intermediate-settings saved far less computational resources than for smaller atoms e.g. chromium or manganese.

In conclusion the three methods discussed earlier can be applied for more new atoms while trying to find the balance between the level of accuracy and the use of the computational resources.

References

[1] S. H. Simon, *The Oxford solid state basics*. 2013. First edition.

[2] D. S. Sholl and J. A. Steckel, *Density Functional Theory: A Practical Introduction*. 2009. DOI:10.1002/9780470447710.

[3] S. Levchenko, X. Ren, J. Wieferink, R. Johanni, P. Rinke, V. Blum, and M. Scheffler, "Hybrid functionals for large periodic systems in an all-electron, numeric atom-centered basis framework." Computer Physics Communications 192, 60-69, 2015. https://doi.org/10.1016/j.cpc.2015.02.021.

[4] X. Ren, P. Rinke, V. Blum, A. T. Jürgen Wieferink, A. Sanfilippo, K. Reuter, and M. Scheffler, "Resolution-of-identity approach to hartree-fock, hybrid density functionals, rpa, mp2, and gw with numeric atom-centered orbital basis functions." New Journal of Physics 14, 053020, 2012.

[5] V. Blum, R. Gehrke, F. Hanke, P. Havu, V. Havu, X. Ren, K. Reuter, and M. Scheffler, *The Fritz Haber Institute ab initio molecular simulations package (FHI-aims)*, 2009.

[6] V. Blum, R. Gehrke, F. Hanke, P. Havu, V. Havu, X. Ren, K. Reuter, and M. Scheffler, "Ab initio molecular simulations with numeric atom-centered orbitals." Computer Physics Communications 180, 2175-2196, 2009. https://doi.org/10.1016/j.cpc.2009.06.022.

[7] https://www.nomad coe.eu. cited 15.8.2018.